Evaluation of modeled surface ozone biases as a function of cloud cover fraction

Hyun Cheol Kim[1,2], Pius Lee[1], Fong Ngan[1,2], Youhua Tang[1,2], Hye Lim Yoo[1,2], and Li Pan[1,2]

[1] NOAA/Air Resources Laboratory, College Park, MD

[2] UMD/Cooperative Institute for Climate and Satellites, College Park, MD

ABSTRACT

A regional air-quality forecast system's model of surface ozone variability based on cloud coverage is evaluated using satellite-observed cloud fraction (CF) information and a surface air-quality monitoring system. We compared CF and daily maximum ozone from the National Oceanic and Atmospheric Administration's National Air Quality Forecast Capability (NOAA NAQFC) with CFs from the Moderate Resolution Imaging Spectroradiometer (MODIS) and the U.S. Environmental Protection Agency's AirNow surface ozone measurements during May to October, 2014. We found that observed surface ozone shows a negative correlation with the MODIS CFs, showing around 1 ppb decrease for 10% MODIS CF change over the Contiguous United States, while the correlation of modeled surface ozone with the model CFs is much weaker, showing only -0.5 ppb per 10% NAQFC CF change. Further, daytime CF differences between MODIS and NAQFC are correlated with modeled surface-ozone biases between AirNow and NAQFC, showing -1.05 ppb per 10% CF change, implying that spatial- and temporal-misplacement of the modeled cloud field might have biased modeled surface ozone-level. Current NAQFC cloud fields seem to have less CFs compared to MODIS cloud fields (mean NAQFC CF = 0.38 and mean MODIS CF = 0.55), contributing up to 35% of surface-ozone bias in the current NAQFC system.

1. INTRODUCTION

Ground-level ozone is a secondary pollutant resulting from photochemical reactions between oxides of nitrogen (NO_x) and volatile organic compounds (VOC) in the presence of solar radiation. While local ozone production is affected by numerous factors, including precursor emissions and meteorological conditions such as temperature and local circulation, ozone photochemistry is photon-limited, and net ozone production shows a direct relationship with changes in UV actinic flux resulting from clouds and aerosols (Dickerson et al., 1997; He and Carmichael, 1999; Jacobson, 1998; Monks et al., 2004). For instance, Lefer et al. (2003) showed that without sufficient UV radiation, ozone production in Houston is limited regardless of local circulation patterns or emission sources. Studies in the urban cities of Los Angeles, California (Jacobson, 1998) and Mexico City (Castro et al., 2001; Raga, Castro et al., 2001), also showed that surface ozone varies from 5% to 30% due to light-absorbing aerosols. Model studies have shown that surface ozone is affected by cloud fields (Voulgarakis et al., 2009; Wild et al., 2000) or strongly scattering aerosols (Dickerson et al., 1997; He and Carmichael, 1999).

Since clouds play a critical role in the radiative balance of the Earth, their impact and models' capabilities to simulate clouds have been repeatedly tested from global and climate

40   perspectives (Bergman and Salby, 1996; Eastman and Warren, 2013; Stephens, 2005). Clouds
41   also play an important role in regional air quality, impacting both surface ozone and particulate
42   matter by regulating photochemical reaction rates, heterogeneous chemistry, and the evolution
43   and partitioning of particulate matter. These impacts, however, still have high measurement
44   uncertainties and are not well quantified. While reliable estimates of photolysis rates are
45   essential for reducing the uncertainty in air-quality modeling, most current models use highly
46   parameterized methods to estimate photolysis rates. Pour-Biazar et al. (2007) argued that the
47   uncertainties in estimation of cloud transmissivity and errors in the placement of clouds'
48   location and time could be an important source of uncertainties in simulations of surface ozone,
49   demonstrating during the Texas Air Quality Study campaign that surface-ozone modeling can be
50   improved by adjusting photolysis rates based on the Geostationary Operational Environmental
51   Satellite cloud product. They also stated that the cloud-prediction problem is particularly
52   frustrating when modeling air quality in State Implementation Plans if they are not able to
53   reproduce satellite-observed cloud fields in a model.

54   In order to reduce computational cost, most regional air-quality models, including the US
55   Environmental Protection Agency (EPA) Community Multi-scale Air Quality model (CMAQ), use a
56   two-step approach for calculating photolysis rates (Byun and Schere, 2006). In preprocessing,
57   the clear-sky photolysis rates for a range of latitudes, altitudes, and solar zenith angles are first
58   computed using a radiative transfer module (Madronich, 1987). Then, within the chemical-
59   transport model, the tabular photolysis rates are interpolated for each location and then
60   adjusted using fractional cloud-coverage information. Since most early meteorological models
61   did not generate the full suite of specific cloud and moisture fields required as input for the
62   chemical-transport model, regional air-quality models were designed to diagnose some
63   additional cloud-related fields from meteorological state variables for use in the chemical-
64   transport model. The Meteorology-Chemistry Interface Processor (MCIP), CMAQ's preprocessor,
65   diagnoses for each horizontal grid cell the cloud coverage, cloud base and top, and the average
66   liquid water content in the cloud using a series of simple algorithms based on a relative-
67   humidity threshold (Otte and Pleim, 2010). For example, in CMAQ modules the photolysis rates
68   below clouds are calculated as:

$$J_{below} = J_{clear}[1 + f_c(1.6 \cdot tr_c \cos(\theta) - 1)] \qquad (1)$$

69   where tr_c is cloud transmissivity, f_c is the cloud fraction for a grid cell, and θ is the solar zenith
70   angle. Cloud fraction is estimated using relative humidity (RH) and critical RH (Byun and Ching,
71   1999). Cloud fraction (f_c^k) above the boundary layer is:

$$f_c^k = \left[\frac{RH^k - RH_c}{1 - RH_c}\right]^2 \qquad (2)$$

72   where RH^k is the relative humidity at vertical model layer k and RH_c is the critical relative
73   humidity defined as $RH_c = 1 - 2\sigma_c(1 - \sigma_c)[1 + 1.732(\sigma_c - 0.5)]$ and $\sigma_c = p^k/p^{k_{PBL}}$ (Geleyn
74   et al., 1982).

75   Within the convective boundary layer when $RH > RH_c$,

$$f_c^k = 0.34 \frac{RH^k - RH_c}{1 - RH_c} \tag{3}$$

76 (Schumann, 1989; Wyngaard and Brost, 1984). See line 131-177 of bcldprc_ak.f90 for MCIP v3.6.

77 Although fractional cloud coverage (i.e., cloud fraction) thus plays a crucial role in determining
78 the final values for photolysis rate, it is not a well-defined physical state variable and is mostly
79 threshold-specific for each retrieval algorithm. One may notice that there are two possible
80 uncertainties in modeling cloud fraction: (1) the model's capability to generate the proper
81 amount of cloud fields, both in their displacement and timing; and (2) conceptual consistency in
82 definitions of cloud fraction between model and observation (i.e., from satellite). In this study,
83 we present efforts to evaluate the cloud-coverage information used in a regional air-quality
84 model through satellite-based cloud fraction information and surface-monitored ozone
85 observations. In the second section, we introduce the observational and modeling data used in
86 this analysis, and results are discussed in Section 3. General performance of the Contiguous
87 United States (CONUS)-scale air-quality forecast system and possible overestimation of surface-
88 ozone levels due to uncertainty in cloud fractions will be also discussed.

89   2. DATA AND METHOD

90 **MODIS:** The Moderate Resolution Imaging Spectroradiometer (MODIS) cloud level 2 product
91 (MOD06_L2 and MYD06_L2, http://modis-atmos.gsfc.nasa.gov/MOD06_L2/index.html) is used
92 for daily cloud-coverage information for each surface-monitoring site. We have retrieved 5-km
93 cloud fraction data, which is based on MOD35_L2 cloud-mask information with 1km and 250m
94 (nadir) spatial resolution. Brightness temperatures (BT) from multiple channels and their
95 differences (BTD) are used in cloud-masking algorithms, as described in the MODIS cloud-mask
96 product (MOD35_L2) user guide (http://modis-atmos.gsfc.nasa.gov/_docs/CMUSERSGUIDE.pdf).
97 For example, daytime land-cloud maskings are determined using BTs and BTDs from 1.38-, 3.7-,
98 3.9-, 6.7-, 8-, 11-, 12-, and 13.9- μm channels. Only data from local afternoon time (~1:30 pm),
99 when ground-level data show high ozone-production efficiency, are used in the analysis.

100 **AirNow:** Real-time ozone measurements across the CONUS are provided by the EPA through the
101 AirNow network (http://www.epa.gov/airnow). From more than 1000 Air Quality System (AQS)
102 sites throughout the CONUS, hourly surface ozone data is obtained, and a daily maximum eight-
103 hour moving averaged ozone (MDA8 ozone) value is calculated for each site.

104 **NAQFC:** The U.S. National Air Quality Forecast Capability (NAQFC) provides daily, ground-level
105 ozone predictions using the Weather Forecasting and Research non-hydrostatic mesoscale
106 model (WRF-NMM) and CMAQ framework across the CONUS with 12-km resolution domain
107 (Chai et al., 2013; Eder et al., 2009). In our analysis, we used the experimental version of NAQFC,
108 which uses WRF-NMM with B-grid (NMMB) as a meteorological driver and the CB05 chemical
109 mechanism. Meteorological data is processed using the PREMAQ, which is a special version of
110 MCIP designed for the NAQFC system. While NAQFC has shown a tendency to overpredict MDA8
111 ozone (Chai et al., 2013), recent updates to model processes and emission have reduced its bias.
112 The "CFRAC" variable from METCRO2D output files are used for cloud fraction.

113 **METHOD:** For each EPA monitoring site and the corresponding model cells, we have calculated a
114 daily maximum of eight-hour, forward-moving, averaged concentrations. For the same

115   locations, we also calculated daytime (~1:30pm local time) cloud fractions from the model and
116   from satellite data. MODIS cloud fractions are regridded into 12-km domain grid cells using a
117   conservative regridding method (Kim et al., 2013). For consistent comparisons, only valid
118   observational data are used, those with corresponding times and locations. We have
119   investigated the six-month summer ozone season (May-October, 2014) and results are
120   consistent for each month.

121   3. RESULTS AND DISCUSSION

122   General distributions of daily and monthly daytime cloud fractions from the model and from
123   satellite are compared. Figure 1 shows the distribution of cloud fractions retrieved from NAQFC
124   and MODIS cloud products (MOD06 level2) for one day (Aug. 2, 2014) in the upper panels; and
125   the figure shows a one-month average (Aug. 2014) in the lower panels. The August 2 plot is
126   overlaid with a NCEP surface-analysis chart to show its association with general features of the
127   synoptic weather pattern. It is obvious that both model and satellite correctly display the
128   general features of cloud coverage associated with the synoptic frontal activities. However,
129   there is a serious discrepancy in their quantity; in most cases the amount of cloud fraction used
130   in the model is smaller than the cloud fraction retrieved from the MODIS cloud product. For
131   August 2014, monthly means of daytime cloud-fractions from NAQFC and MODIS are 0.38 and
132   0.55, respectively.

133   This discrepancy becomes even more evident from the histogram distribution. In Figure 2, we
134   present histogram distributions of cloud fractions from NAQFC and from MODIS during August
135   2014 for each 0.1 cloud-fraction bin. Occurrence frequency is shown on the y-axis, so the sum of
136   total frequency makes 100%. In the NAQFC model, lower cloud-fraction numbers are more
137   dominant, with the highest frequency between 0.2 and 0.3, showing very low frequency of high
138   cloud fractions. On the other hand, the MODIS cloud fraction is quite different, showing more of
139   a bimodal distribution. Frequencies for clear sky are similar between the model and satellite,
140   around 12–13%, but the satellite cloud frequency is much lower in the 0.1–0.5 range and higher
141   above 0.6.

142   The reason for this discrepancy between the model and MODIS is not clear and requires future
143   investigation. As mentioned previously, this might be a characteristic of the meteorological
144   model or it could be a conceptual difference in cloud fraction between model and satellite. As
145   cloud-fraction field is a diagnosed variable in PREMAQ, which uses a certain threshold of liquid-
146   water content or relative humidity to model the existence of clouds, it may differ from the
147   satellite's measurements of cloud, which uses emissivity-based cloud masking using BT and BTD
148   from multiple channels.

149   Figures 3a and 3b show scatter plots between MODIS cloud fractions and AirNow MDA8 ozone
150   and between NAQFC cloud fractions and MDA8 ozone, respectively, during August 1024 across
151   all reporting EPA AQS monitoring-sites. As the amount of UVA (ultraviolet radiation in 315-399
152   nm) strongly affects the ozone production by NO_2 photodissociation (e.g. j(NO2) in $\lambda < 420$ nm)
153   at the surface, it is evident that cloud fraction, and the eventual flux of photons reaching the
154   level of the surface, is a very dominant component determining ground-level ozone
155   concentration (Monks et al., 2004; Seinfeld and Pandis, 2006). Scatter plots in Figure 3a draw
156   data from more than 1000 sites across the CONUS under a variety of meteorological conditions
157   and precursor sources. Even with the high uncertainties here, we can see a notable separation

158 of ground-level ozone for each cloud-fraction bin, implying that photon flux is one of the most
159 dominant features determining tropospheric ozone photochemistry. Slope and offsets for line-
160 fitting MODIS CF versus AirNow MDA8 ozone are -11.33 and 49, respectively, implying that 10%
161 of CF change can cause around 1.13 ppb decrease in surface ozone. On the other hand, the
162 correlation between NAQFC CF and MDA8 ozone is slightly weaker (Figure 3b); slope and offsets
163 between NAQFC CF and MDA 8 ozone are -5.0 and 50.5, respectively, showing half as much
164 sensitivity in surface ozone according to the NAQFC CF compared to the MODIS CF.

165 Figures 3c and 3d are scatter plots for CF differences (NAQFC-MODIS) and MDA8 surface ozone
166 bias (NAQFC-AQS; left), and averaged O_3 biases for each 0.1 cloud-fraction bin (right). Since the
167 definition of cloud fraction in the model and the satellite are slightly different, we choose the
168 term "cloud fraction difference" instead of "cloud fraction bias." Slope of the linear regression is
169 -10.5 ppb/100% CF. The right-side panel shows averages of ozone biases for each 0.1 bin. The
170 vertical bars indicate 1 standard deviation. It is clear that where the model underestimates
171 cloud fraction, it likely overestimates surface ozone, although there are many intricacies of
172 tropospheric ozone chemistry involved.

173 Since Figure 3 shows data from all AQS sites, it includes multiple uncertainties from each site's
174 local characteristics, such as local emissions. We have conducted further investigation for
175 individual AQS sites to confirm if we can find similar MDA8 ozone to CF correlation. Figure 4
176 shows spatial distributions of each site's ozone to CF sensitivity (e.g., regression slope of MDA8
177 ozone and CF) and correlation coefficients during 5 months (May to September, 2014). MDA8
178 ozone decreases rapidly by the increase of CF in the southern regions, especially near the
179 coastal lines of Gulf of Mexico, such as Texas, Louisiana and Florida, up to -30 ppb/CF. In the
180 middle latitude regression slopes are around -10 ppb/CF, and some northern location areas
181 show positive correlation. Mean of total regression slope is -8.5 ppb/CF. Correlation coefficients
182 (R) also show stronger (negative) correlation in southern states, especially southeastern US up
183 to R=-0.7 while northeastern US shows much weaker correlation, implying accurate CF
184 information is important in southern US states.

185 **OZONE OVERPREDICTION** : As already described, current NAQFC cloud fields seem to   have
186 fewer clouds than MODIS by 0.2. We have further estimated how this difference can affect the
187 general performance of surface ozone forecast. Previous studies address O_3 overpredictions of
188 global and regional chemical-transport models during the summer daytime over the eastern
189 United States (Chai et al., 2013; Eder et al., 2009; Fiore et al., 2009; Murazaki and Hess, 2006;
190 Nolte et al., 2008; Rasmussen et al., 2012; Reidmiller et al., 2009). Studies have addressed that
191 the vertical resolution (Murazaki and Hess, 2006), the coarse representation of emissions (Liang
192 and Jacobson, 2000), along with uncertainty in the heterogeneous reactions of aerosols (Martin
193 et al., 2003) contribute to the highly biased O_3 of the global chemical-transport models MOZART
194 or GEOS-Chem over the eastern United States. NAQFC also has a tendency to overestimate
195 surface ozone during ozone season. We may estimate the amount of possible overestimation of
196 surface ozone due to the underestimation of the cloud fraction and eventual overestimation of
197 photolysis rate. As the mean cloud fraction of model is 0.17 higher than the cloud-fraction
198 estimated from MODIS, by applying the -10.5 ppb/CF estimate, we can deduce that 1.8 ppb of
199 the surface-ozone overestimation is contributed from the underestimation of the cloud fraction.
200 Considering current NAQFC surface-ozone overestimation is around 5 ppb for the month of
201 August 2014, we can roughly suggest that almost 35% of this overestimation is due to faulty
202 estimation of the cloud field. Though this estimate is still very rough, this is definitely something

203 to consider carefully in order to improve the simulation of regional air quality and especially the
204 simulation of surface ozone.

205 **RESOLUTION ISSUE**: In utilizing satellite-based cloud-fraction information, one concern is how to
206 process data in terms of pixel resolution. As already mentioned, the cloud fraction is not a state
207 variable; it is threshold- or retrieval-specific. For example, if we consider an area with 9 pixels
208 with cloud fraction 0.6, fractional averaging of 9 cloud pixels should yield a 0.6 cloud fraction.
209 However, if we first perform cloud masking for each pixel, we may have 9 cloud markings out of
210 9 pixels, resulting in 100% cloud fraction. This might not be a critical error on a global scale, but
211 it is a crucial difference for regional or local scales intended for investigating the spatial scale of
212 local ozone production. Since cloud fields are very localized phenomena, this information should
213 be processed as finely as data are available.

214 To conclude, this study demonstrates that appropriate model of CF is crucial in the modeling of
215 surface ozone chemistry. Further studies are needed in terms of the comparison of modeled- or
216 satellite-based CF with actual surface level photon flux, as well as enhanced parameterization of
217 CF in the air quality model.

218   4.   REFERENCES

219 Bergman, J. W., and Salby, M. L. (1996). Diurnal variations of cloud cover and their relationship
220   to climatological conditions. *Journal of Climate*, *9*(11), 2802–2820.

221 Byun, D., and Schere, K. L. (2006). Review of the Governing Equations, Computational
222   Algorithms, and Other Components of the Models-3 Community Multiscale Air Quality
223   (CMAQ) Modeling System. *Applied Mechanics Reviews*, *59*(2), 51. doi:10.1115/1.2128636

224 Byun, D. W., and Ching, J. K. S. (1999). *Science Algorithms of the EPA Models-3 Community*
225   *Multiscale Air Quality (CMAQ) Modeling System*. Washington, DC, USA: US Environmental
226   Protection Agency, Office of Research and Development.

227 Castro, T., Madronich, S., Rivale, S., Muhlia, A., & Mar, B. (2001). The influence of aerosols on
228   photochemical smog in Mexico City. *Atmospheric Environment*, *35*(10), 1765–1772.
229   doi:10.1016/S1352-2310(00)00449-0

230 Chai, T., Kim, H.-C., Lee, P., Tong, D., Pan, L., Tang, Y., Huang J., McQueen, J., Tsidulko, M., and
231   Stajner, I. (2013). Evaluation of the United States National Air Quality Forecast Capability
232   experimental real-time predictions in 2010 using Air Quality System ozone and NO_2
233   measurements. *Geoscientific Model Development*, *6*(5), 1831–1850. doi:10.5194/gmd-6-
234   1831-2013

235 Dickerson, R. R., Kondragunta, S., Stenchikov, G., Civerolo, K. L., Doddridge, B. G., and Holben, B.
236   N. (1997). The Impact of Aerosols on Solar Ultraviolet Radiation and Photochemical Smog.
237   *Science*, *278*(5339), 827–830. doi:10.1126/science.278.5339.827

238 Eastman, R., and Warren, S. G. (2013). A 39-yr survey of cloud changes from land stations
239   worldwide 1971-2009: Long-term trends, relation to aerosols, and expansion of the
240   tropical belt. *Journal of Climate*, *26*(4), 1286–1303.

241   Eder, B., Kang, D., Mathur, R., Pleim, J., Yu, S., Otte, T., and Pouliot, G. (2009). A performance
242   evaluation of the National Air Quality Forecast Capability for the summer of 2007☆.
243   *Atmospheric Environment*, *43*(14), 2312–2320. doi:10.1016/j.atmosenv.2009.01.033

244   Fiore, a. M., Dentener, F. J., Wild, O., Cuvelier, C., Schultz, M. G., Hess, P., … Zuber, a. (2009).
245   Multimodel estimates of intercontinental source-receptor relationships for ozone pollution.
246   *Journal of Geophysical Research*, *114*(D4), 10816. doi:10.1029/2008JD010816

247   Geleyn, J. F., Hense, A., and Preuss, H. J. (1982). A comparison of model generated radiation
248   fields with satellite measurements. *Beitr. Phys. Atmos.*, *55*, 253–286.

249   He, S., and Carmichael, G. R. (1999). Sensitivity of photolysis rates and ozone production in the
250   troposphere to aerosol properties. *Journal of Geophysical Research*, *104*(D21), 26307.
251   doi:10.1029/1999JD900789

252   Jacobson, M. Z. (1998). Studying the effects of aerosols on vertical photolysis rate coefficient
253   and temperature profiles over an urban airshed. *J. of Geophys. Res.*, *103*(D9), 10593.
254   doi:10.1029/98JD00287

255   Kim, H., Ngan, F., Lee, P., and Tong, D. (2013). *Development of IDL-based geospatial data*
256   *processing framework for meteorology and air quality modeling*. Retrieved from
257   http://aqrp.ceer.utexas.edu/projectinfoFY12_13%5C12-TN2%5C12-TN2 Final Report.pdf

258   Lefer, B. L. (2003). Impact of clouds and aerosols on photolysis frequencies and photochemistry
259   during TRACE-P: 1. Analysis using radiative transfer and photochemical box models. *Journal*
260   *of Geophysical Research*, *108*(D21), 8821. doi:10.1029/2002JD003171

261   Liang, J., and Jacobson, M. Z. (2000). Effects of subgrid segregation on ozone production
262   efficiency in a chemical model. *Atmospheric Environment*, *34*(18), 2975–2982.
263   doi:10.1016/S1352-2310(99)00520-8

264   Madronich, S. (1987). Photodissociation in the atmosphere: 1. Actinic flux and the effects of
265   ground reflections and clouds. *Journal of Geophysical Research*, *92*(D8), 9740.
266   doi:10.1029/JD092iD08p09740

267   Martin, R. V., Jacob, D. J., and Yantosca, R. M. (2003). Global and regional decreases in
268   tropospheric oxidants from photochemical effects of aerosols. *Journal of Geophysical*
269   *Research*, *108*(D3), 4097. doi:10.1029/2002JD002622

270   Monks, P. S. (2004). Attenuation of spectral actinic flux and photolysis frequencies at the surface
271   through homogenous cloud fields. *Journal of Geophysical Research*, *109*(D17), D17206.
272   doi:10.1029/2003JD004076

273   Murazaki, K., and Hess, P. (2006). How does climate change contribute to surface ozone change
274   over the United States? *Journal of Geophysical Research*, *111*(D5), D05301.
275   doi:10.1029/2005JD005873

276 Nolte, C. G., Gilliland, A. B., Hogrefe, C., and Mickley, L. J. (2008). Linking global to regional
277   models to assess future climate impacts on surface ozone levels in the United States.
278   *Journal of Geophysical Research*, *113*(D14), D14307. doi:10.1029/2007JD008497

279 Otte, T. L., and Pleim, J. E. (2010). The Meteorology-Chemistry Interface Processor (MCIP) for
280   the CMAQ modeling system: updates through MCIPv3.4.1. *Geoscientific Model*
281   *Development*, *3*(1), 243–256. doi:10.5194/gmd-3-243-2010

282 Pour-Biazar, A., McNider, R. T., Roselle, S. J., Suggs, R., Jedlovec, G., Byun, D. W., … Cameron, R.
283   (2007). Correcting photolysis rates on the basis of satellite observed clouds. *Journal of*
284   *Geophysical Research*, *112*(D10), D10302. doi:10.1029/2006JD007422

285 Raga, G., Castro, T., and Baumgardner, D. (2001). The impact of megacity pollution on local
286   climate and implications for the regional environment: Mexico City. *Atmospheric*
287   *Environment*, *35*(10), 1805–1811. doi:10.1016/S1352-2310(00)00275-2

288 Rasmussen, D., Fiore, A., Naik, V., Horowitz, L. W., McGinnis, S. J., and Schultz, M. G. (2012).
289   Surface ozone-temperature relationships in the eastern US: A monthly climatology for
290   evaluating chemistry-climate models. *Atmospheric Environment*, *47*, 142–153.
291   doi:10.1016/j.atmosenv.2011.11.021

292 Reidmiller, D. R., Fiore, a. M., Jaffe, D. a., Bergmann, D., Cuvelier, C., Dentener, F. J., … Zuber, A.
293   (2009). The influence of foreign vs. North American emissions on surface ozone in the US.
294   *Atmospheric Chemistry and Physics*, *9*(14), 5027–5042. doi:10.5194/acp-9-5027-2009

295 Schumann, U. (1989). Large-eddy simulation of turbulent diffusion with chemical reactions in
296   the convective boundary layer. *Atmospheric Environment (1967)*, *23*(8), 6981. Retrieved
297   from http://www.sciencedirect.com/science/article/pii/0004698189900565

298 Seinfeld, J. H., and Pandis, S. N. (2006). *Atmospheric Chemistry and Physics* (p. 1232).

299 Stephens, G. L. (2005). Cloud feedbacks in the climate system: A critical review. *Journal of*
300   *Climate*.

301 Voulgarakis, A., Wild, O., Savage, N. H., Carver, G. D., and Pyle, J. A. (2009). Clouds, photolysis
302   and regional tropospheric ozone budgets. *Atmospheric Chemistry and Physics*, *9*(21), 8235–
303   8246. doi:10.5194/acp-9-8235-2009

304 Wild, O., Zhu, X., and Prather, M. (2000). Fast-J: Accurate simulation of in-and below-cloud
305   photolysis in tropospheric chemical models. *Journal of Atmospheric Chemistry*, 2000.
306   doi:10.1023/A:1006415919030

307 Wyngaard, J., and Brost, R. (1984). Top-down and bottom-up diffusion of a scalar in the
308   convective boundary layer. *Journal of the Atmospheric Sciences*, *41*, 102–112.
309   doi:http://dx.doi.org/10.1175/1520-0469(1984)041<0102:TDABUD>2.0.CO;2

310

311

312
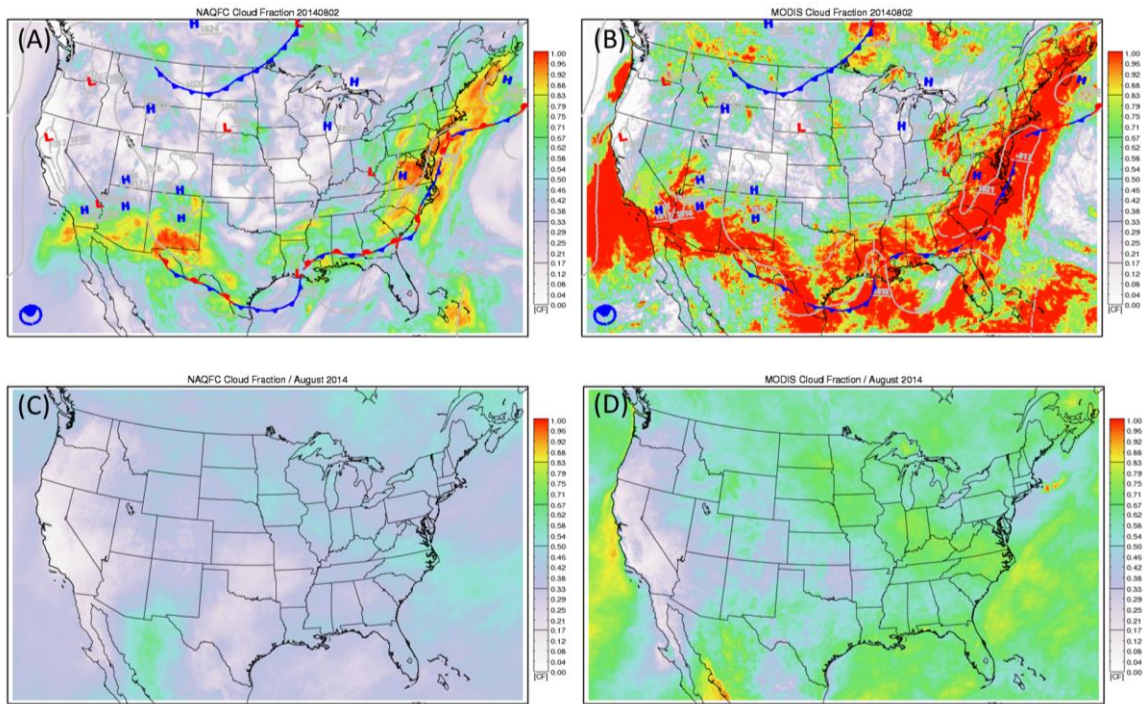
Figure 1. Spatial distributions of cloud fractions on Aug. 2, 2014 from NAQFC (a) and MODIS (b).
NOAA NCEP surface weather chart at 18UTC is overlaid. Monthly averaged distributions are also
shown for NAQFC (c) and MODIS (d).

MODIS & NAQFC Cloud Fraction / August 2014
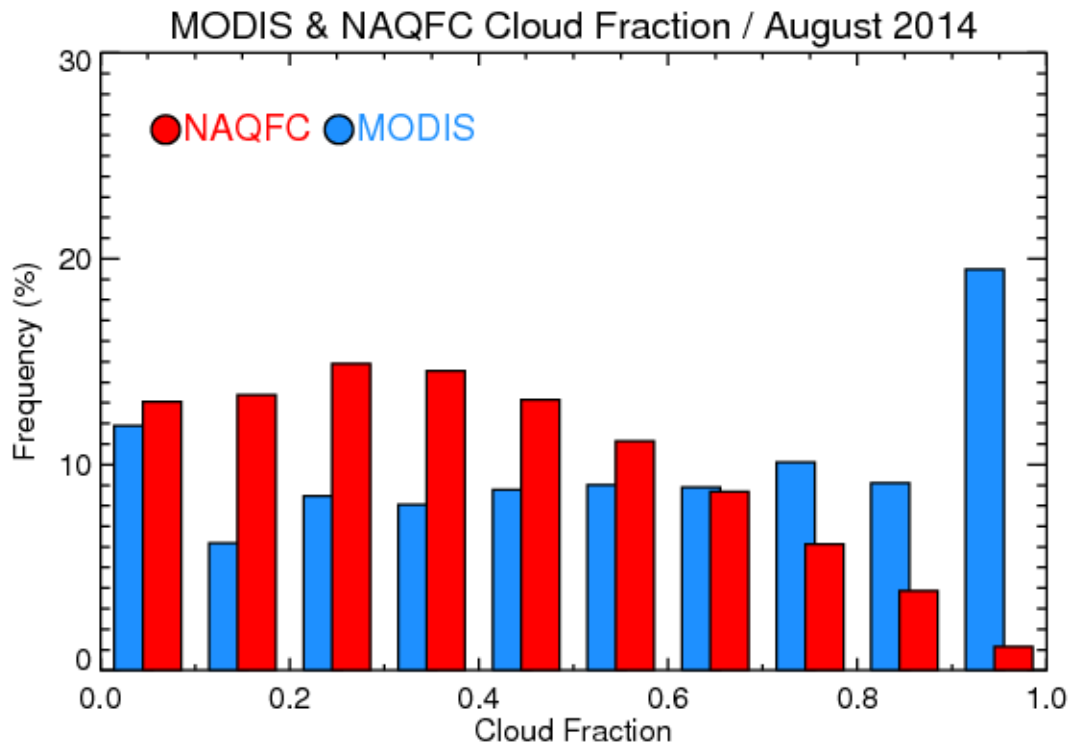
319
320   Figure 2. Occurrence frequency histogram for NAQFC cloud fractions (red) and MODIS cloud
321   fractions (blue).
322
323

324
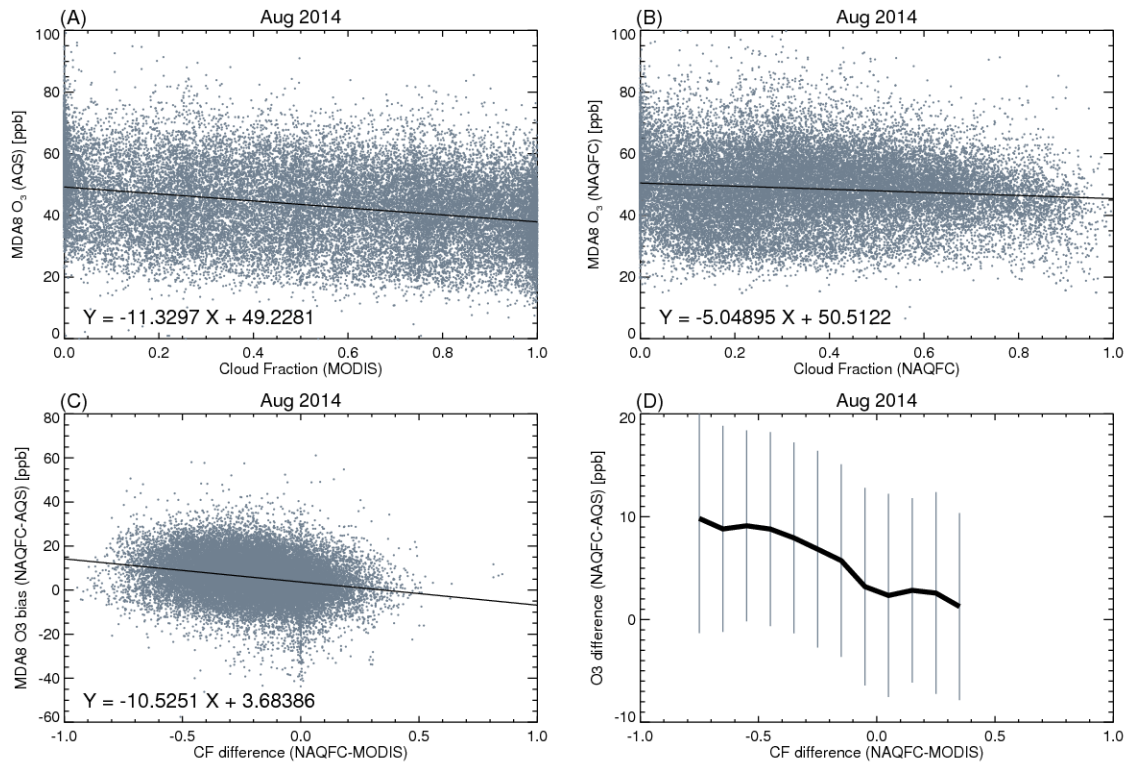
325
326
327 Figure 3. Scattered plots between MODIS cloud fractions and AQS MDA8 ozone (a), between
328 NAQFC cloud fractions and MDA8 ozone (b), and between cloud fraction differences (NAQFC -
329 MODIS) and MDA8 surface ozone bias (NAQFC-AQS) (c) during Aug. 2014 across 1024 AQS
330 monitoring site locations. Averaged O_3 biases for each 0.1 cloud-fraction bin with 1 standard
331 deviation (vertical bars) are also shown (d).
332
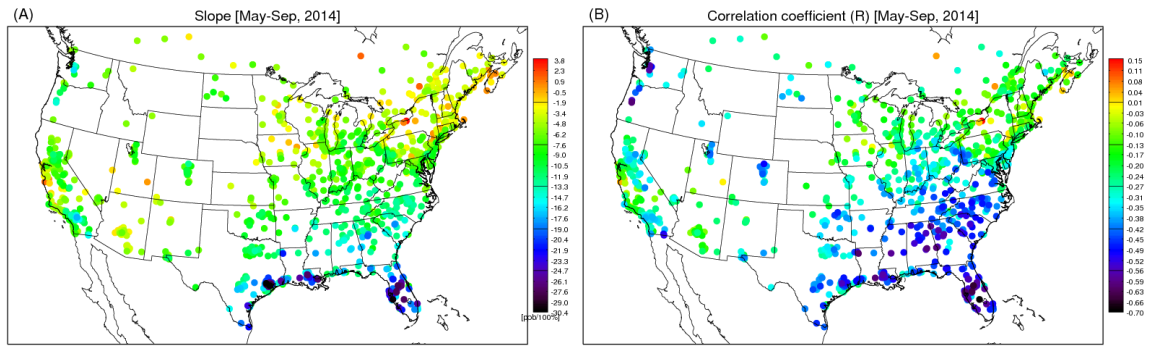
333
334 Figure 4. Spatial distributions of (a) slope and (b) correlation coefficient of linear regression
335 between MODIS CF and MDA8 ozone.